Journal of Power Sources 260 (2014) 307–316

Contents lists available at ScienceDirect

Journal of Power Sources

journal homepage: www.elsevier.com/locate/jpowsour

Preparation and characterization of sulfonated poly(arylene ether ketone) copolymers with pendant sulfoalkyl groups as proton exchange membranes

Hailong Cheng [a], Jingmei Xu [a], Li Ma [a], Lishuang Xu [a], Baijun Liu [a], Zhe Wang [a,b,*], Huixuan Zhang [a]

[a] Engineering Research Center of Synthetic Resin and Special Chemical Fiber, Changchun University of Technology, Changchun 130012, PR China
[b] Advanced Institute of Materials Science, Changchun University of Technology, Changchun 130012, PR China

HIGHLIGHTS

- A series of novel SPAEK copolymers with pendant sulfoalkyl groups are prepared.
- Direct copolymerization method can control the polymer structures precisely.
- These membranes show a higher relative selectivity due to the special structure.
- A higher relative selectivity is sufficient to achieve improved PEMFC performance.

ARTICLE INFO

Article history:
Received 13 November 2013
Received in revised form
21 February 2014
Accepted 6 March 2014
Available online 19 March 2014

Keywords:
Sulfonated poly (aryl ether ketone)
Pendant
Proton exchange membrane
Fuel cell

ABSTRACT

A series of novel sulfonated poly(arylene ether ketone) (SPAEK) copolymers with pendant sulfoalkyl groups are prepared via nucleophilic polycondensation reactions. The sulfonate content of the SPAEK copolymers can be controlled easily by adjusting the ratio of the sulfonated and unsulfonated monomer feeds. The structures of the synthesized sulfonated copolymers are confirmed by ^{1}H NMR and Fourier transform infrared spectra. The microstructures of the membranes are investigated by transmission electron microscopy. Mechanical properties, thermal and oxidative stabilities, water uptake, swelling ratio, proton conductivity, and methanol permeability of the membranes are systematically investigated. The results demonstrated that the membranes have good performance. The proton conductivities of the side-chain-type SPAEK-100 membrane reach 0.051 and 0.152 S cm^{-1} at 25 and 120 °C, respectively. The methanol permeabilities of the side-chain-type SPAEK membranes are in the range of 0.12×10^{-7}–3.55×10^{-7} m^2 s^{-1}, which is lower than that of the Nafion 117 membrane, i.e., 23.8×10^{-7} m^2 s^{-1}. A higher relative selectivity than that of Nafion 117 is also observed. These results indicate that there is a great potential for side-chain-type SPAEK membranes to be used in proton exchange membrane fuel cell applications.

1. Introduction

Proton exchange membrane fuel cells (PEMFCs) have been extensively investigated due to their high efficiency, renewability, and low environmental cost [1,2]. Direct methanol fuel cells (DMFCs), a type of PEMFC, have been widely used in many fields such as transportation, aerospace, and as mobile power stations [3,4]. As one of the primary components in DMFCs, proton exchange membranes (PEMs) not only help in the transfer of protons, but also acts as a barrier between the gases/fuels and oxidant between the electrodes [5,6]. Currently, perfluorosulfonic acid membranes such as Nafion are the most widely used materials for PEMFCs owing to their excellent mechanical properties, long-term durability, and outstanding proton conductivity. However, there are disadvantages, such as the high production cost, low conductivity at high temperature (>80 °C), and high methanol permeability, which hinder further applications of the perfluorosulfonic acid membranes [7]. Consequently, alternative materials for PEMFCs are being developed [8,9].

* Corresponding author. Engineering Research Center of Synthetic Resin and Special Chemical Fiber, Changchun University of Technology, Changchun 130012, PR China. Tel./fax: +86 431 85716465.
E-mail address: wzccut@126.com (Z. Wang).

http://dx.doi.org/10.1016/j.jpowsour.2014.03.023
0378-7753/

In recent years, sulfonated aromatic polymers such as sulfonated poly(arylene ether ketone) [10,11], sulfonated poly(ether sulfone) [12–15], sulfonated polyimide [16,17], sulfonated polybenzimidazole [18,19], and sulfonated poly(ether amide) [20] have been extensively studied as alternative materials owing to their excellent thermal and chemical stability, mechanical properties, and relatively low production cost. However, the sulfonic acid groups in these main-chain-type sulfonated aromatic polymers are directly attached to the rigid backbone of the polymers; therefore, these polymers are unable to form pronounced microphase-separated structures and have more dead-end channels compared to Nafion [21]. In general, these main-chain-type polymers only achieve suitable conductivities at high ion exchange capacity (IEC) and high water contents. High IECs lead to excess water uptake, thereby causing large dimensional variations and loss of mechanical properties. To overcome these drawbacks of main-chain-type polymers, hydrophilic sulfonic acid groups are separated from the hydrophobic main chains by locating them far away on the side chains [22,23]. By doing this, it is possible to attribute the excellent thermal, mechanical, and electrochemical properties of Nafion to a typical microphase-separated structure [24]. To achieve the desired microphase-separated structure, many side-chain-type sulfonated polymers have been developed as described below. Side-chain-type sulfonated polysulfones with attractive membrane properties were synthesized by Jannasch et al. via lithiation of polysulfones followed by an anionic reaction with sulfobenzoic acid cyclic anhydride [23,25]. Side-chain-type sulfonated aromatic derivatives with excellent proton conductivities under relatively low water contents were synthesized by Guiver and coworkers [26,27]. Furthermore, side-chain-type sulfonated polyimides with high proton conductivities and outstanding dimensional stability were synthesized by Miyatake et al. [28].

In this study, a novel sulfonated monomer 4-(4-(4-(2,5-dihydroxyphenyl)-aniline acyl)anilino)-butane-1-sulfonic acid (4-DABS) was initially synthesized, and then a series of novel side-chain-type sulfonated poly(arylene ether ketone) (SPAEK) copolymers were synthesized by nucleophilic polycondensation of 4-DABS, 4,4-difluorobenzophenone (DFB), and 2,2′-bis(4-hydroxyphenyl)propane (BPA). Compared to chemical grafting and post-sulfonation methods, direct copolymerization of the respective monomers can precisely control the sulfonate content in the copolymers, and thereby facilitate the study of their structure–property relationships. Herein, thermal and mechanical properties, water uptake and swelling behavior, water diffusion coefficients, methanol permeability, and proton conductivity of the membrane materials were systematically investigated.

2. Experimental

2.1. Materials

DFB was purchased from Longjing Chemical Plant. 1,4-Butanesultone, 4-nitroaniline, 4-aminobenzoic acid, BPA, and 1,4-benzoquinone were purchased from J&K Chemical. Triphenyl phosphite (TPP), tetramethylene sulfone (TMS), and 1-methyl-2-pyrrolidinone (NMP) were obtained from Aladdin Reagent Co., Ltd., China. Other reagents were obtained from Beijing Chemical Company and used as received without further purification.

2.2. Synthesis of (4-amino)phenylhydroquinone (4-AmPHQ) and 4-DABS

4-AmPHQ was synthesized through a two-step coupling–reduction reaction, as reported by Liu et al. [29]. 4-Aminobenzoic acid (1.340 g, 9.775 mmol) and 1,4-butanesultone (1 mL, 9.775 mmol) were dissolved in 30 mL NMP in a 100 mL three-neck flask equipped with a mechanical stirrer and condenser, and the reaction mixture was stirred at 75 °C using a water bath for 24 h. Next, 4-AmPHQ (1.965 g, 9.775 mmol) was added into the three-neck flask, followed by 10 mL of TPP. The solution was stirred at 100 °C for 12 h under a nitrogen atmosphere, and then cooled to room temperature and poured into 500 mL of acetone to precipitate the target product. The obtained product was washed with acetone several times, then filtered and dried at 80 °C under a vacuum for 12 h (Scheme 1).

2.3. Synthesis of SPAEK copolymers

A series of SPAEK copolymers with different degrees of sulfonation were synthesized via nucleophilic substitution polycondensation. As an example, the synthesis of SPAEK-80 is described below; where 80 refer to the molar ratio of 4-DABS to the bisphenol monomer. In a 100 mL three-neck round-bottom flask equipped with a Dean–Stark trap, a mechanical stirrer, and a nitrogen inlet, 2.18 g (10 mmol) DFB, 3.584 g (8 mmol) 4-DABS, 0.456 g (2 mmol) BPA, anhydrous K_2CO_3 1.656 g (12 mmol), TMS (19 mL), and toluene (15 mL) were added. The reaction mixture was heated to 130 °C and kept at 130 °C for 4 h to remove the water by azeotropic distillation with toluene. Next, the toluene was evaporated, and the reaction temperature was slowly raised to 170 °C and then maintained for several hours until the solution viscosity increased dramatically (Scheme 2). The mixture was then cooled to ambient temperature, diluted with TMS, and slowly poured into deionized water to obtain the fibrous copolymer. The resulting product was washed with hot deionized water several times to remove impurities and dried under a vacuum at 100 °C for 24 h.

2.4. Membrane preparation

The dried SPAEK copolymers were dissolved in NMP to form 10–15% homogeneous transparent solutions. The copolymer solutions were filtered and then cast onto clean glass substrates. The films were placed in a vacuum oven for 48 h at 150 °C to remove residual solvents. Next, the films were soaked in deionized water to enable removal from the glass substrates; thus, tough and flexible films were obtained. The thicknesses of the membranes were controlled in the range of 60–70 μm.

2.5. Characterization and measurements

FT-IR measurements were obtained using a Nicolet Avatara-360 spectrometer, at a range of frequencies from 4000 to 400 cm^{-1}. The ^1H NMR spectrum was measured on a Bruker Avance spectrometer with deuterated dimethyl sulfoxide (DMSO-d_6) as the solvent and tetramethylsilane as the internal reference standard. The inherent viscosities of the synthesized copolymers were determined with a polymer concentration of 0.5 g dL^{-1} in NMP at 25 °C using an Ubbelohde capillary viscometer. Thermogravimetric analysis (TGA) and differential scanning calorimetry (DSC) were used to evaluate the thermal stability of the membranes. The TGA measurements were performed with a Perkin Elmer Pyris 1 thermal analyzer under an air atmosphere at a heating rate of 10 °C min^{-1}. The DSC measurements were performed using a Mettler Toledo DSC821e instrument under a nitrogen atmosphere at a heating rate of 10 °C min^{-1}. The mechanical properties of the membranes were measured at room temperature with an Instron-5965 at a test speed of 1 mm min^{-1}. The size of the tested specimen was 20 × 4 mm. Each data item was obtained as an average value of at least three tests. Transmission electron microscopy (TEM) images were obtained using a JEM-1011 instrument. In order to obtain the

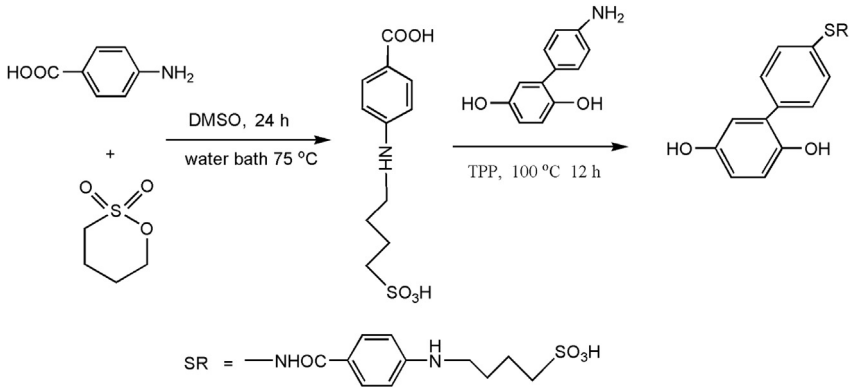

Scheme 1. Synthesis of 4-(4-(4-(2,5-dihydroxyphenyl)-aniline acyl)anilino)-butane-1-sulfonic acid.

corresponding Ag^+ forms of the copolymer proton forms they were immersed in $AgNO_3$ solutions before the tests. The Ag^+ form of the SPAEKs in DMF solutions was cast onto copper grids and then dried at room temperature for 24 h before TEM analysis.

The oxidative stability of the membranes was evaluated by recording the retained weight (RW) of a small piece of the sample after treatment with Fenton's reagent (3% H_2O_2, 2 ppm $FeSO_4$) at 80 °C for 1 h. The ion exchange capacity (IEC) values of the membranes were determined by classical acid–base titration. The H^+ ions in the membrane were liberated by immersing in 2 M NaCl solution for 48 h. The H^+ ions within the solutions were titrated with an aqueous 0.01 M NaOH solution using phenolphthalein as the indicator. At least three experiments were conducted for each measurement until the titration reached a constant value. The IEC values of the SPAEK membranes were measured as follows:

$$\text{IEC} = \frac{\text{consumed (NaOH)} \times \text{molarity (NaOH)}}{\text{mass dried membrane}} \quad (1)$$

The water uptake and swelling ratio were measured from the changes in weight and length between the dry and hydrated membranes at the desired temperature. The membranes were dried under a vacuum at 100 °C for 24 h until a constant weight was obtained and then soaked in deionized water to reach equilibrium at the desired temperatures. The weights and lengths of the dry and wet membranes were measured. The water uptake (WU) of the SPAEK membranes was measured as follows:

$$\text{Water uptake (\%)} = \frac{W_{\text{wet}} - W_{\text{dry}}}{W_{\text{dry}}} \times 100\% \quad (2)$$

where W_{wet} and W_{dry} are the weights of the wet and dried membranes, respectively. The swelling ratio of the SPAEK membranes was measured as follows:

$$\text{Swelling ratio (\%)} = \frac{L_{\text{wet}} - L_{\text{dry}}}{L_{\text{dry}}} \times 100\%$$

$$\text{Swelling ratio (\%)} = \frac{T_{\text{wet}} - T_{\text{dry}}}{T_{\text{dry}}} \times 100\% \quad (3)$$

where L_{wet} and L_{dry} are the lengths of the wet and dry membranes, T_{wet} and T_{dry} are the thickness of the wet and dry membranes, respectively.

The relative hydrophilicity/hydrophobicity of the membranes could be determined easily by contact angle measurements using a DSA 30I drop shape analysis system (Krüss, Germany) at room temperature [30]. Deionized water (2.0 μL) was dropped onto the sample surfaces for these measurements.

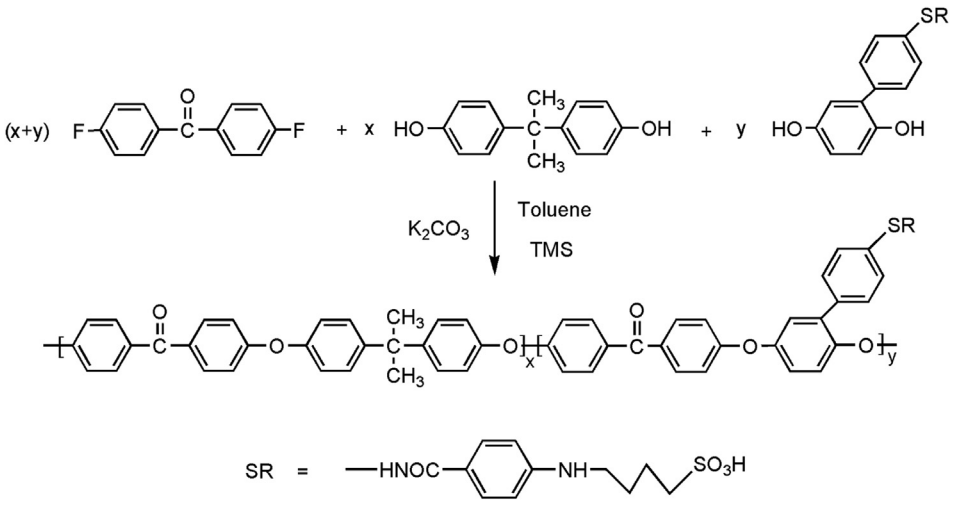

Scheme 2. Synthesis of side-chain-type SPAEK-xx copolymers.

The water diffusion coefficient measurement of the SPAEK membranes was accomplished by a method similar to that reported previously [31], and was calculated by the following formula:

$$\frac{M_t}{M_\infty} = 4\left(\frac{Dt}{\pi L^2}\right)^{1/2} \quad (4)$$

where D is the water diffusion coefficient, M_t/M_∞ is the water desorption, and L is the membrane thickness.

The proton conductivity in the plane direction of the membranes was measured by ac impedance spectroscopy (Philips 1260 impedance/gain-phase analyzer) over a frequency range from 10 Hz to 1 MHz. A sheet of the prepared membrane (15 mm × 10 mm) was placed in a test cell [31] and then fully hydrated in deionized water at the desired temperature for at least 24 h prior to the test. The conductivity measurements of fully hydrated membranes were carried out in water vapor with 100% relative humidity (RH). This experimental setup allowed the membranes to equilibrate with saturated water vapor at the desired temperature. The temperature was controlled by a wrap-around resistance heater and feed back temperature controller. The sample resistance (R) was estimated by extrapolation of the high-frequency arc crossing to the real axis from the impedance plot which obtained from impedance measurement comprises a depressed semicircular arc at high frequency and a spur at low frequency [32]. The proton conductivity of the SPAEK membranes in the plane direction was measured as follows:

$$\sigma = \frac{L}{R \times S} \quad (5)$$

where L is the distance between the two electrodes, R is the membrane resistance, and S is the cross-sectional area of the membrane.

The methanol diffusion coefficient was determined using a liquid permeability cell, which basically consisted of two-half-cells separated by the membrane. Diffusion cell A was filled with methanol solution (10 mol L^{-1}), and diffusion cell B was filled with pure water. The solutions were magnetically stirred to ensure uniformity during the test. The methanol concentrations in the water cell were monitored at different temperatures using a Shimadzu GC-8A chromatograph. The methanol permeability of the SPAEK membranes was calculated as follows [33]:

$$C_B(t) = \frac{A}{V_B}\frac{DK}{L}C_A(t - t_o) \quad (6)$$

where A (in cm^2), L (in cm) and V_B (in mL) are the effective area, thickness of the membranes, and volume of permeated reservoirs, respectively. C_A and C_B (in mol m^{-3}) are the methanol concentration in the methanol and water reservoirs, respectively, and DK (in $cm^2\ s^{-1}$) is the methanol diffusion coefficient.

The fuel cell performances of SPAEK membranes were studied with polarization curves in a single cell test by using a G50 Fuel Cell Test Station from Green Light Company. The catalyst layer (40 wt.% Pt/C, Johnson Matthey) was transferred on the each sides of the membrane to form the catalyst coated membrane (CCM). The loading of the catalyst layer was 0.2 mg Pt cm^{-2} for the anode and cathode. A 20 wt.% wet-proofed Toray carbon paper composed of PTFE and carbon powder on the surface of carbon paper (TGPH-060, Toray Inc.) was used as a gas diffusion layer (GDL) for the anode and cathode sides. The GDL was placed on the two sides (anode and cathode) of the CCM, and then the membrane electrode assembly (MEA) with an active area of 25 cm^2 was prepared by hot pressing method. H_2 and air were supplied at a flow rate of 300 sccm and 2000 sccm, respectively. The measurement was at 100 °C cell temperatures under 100% relative humidity conditions state.

3. Results and discussion

3.1. Structural characteristics

The structures of monomers were characterized by their ^{1}H NMR spectra. 4-AmPHQ was synthesized through a two-step coupling–reduction reaction. Fig. 1a shows the ^{1}H NMR spectra of 4-AmPHQ. The peaks at δ 8.55 and 8.43 ppm were assigned to the protons of hydroxyl groups, and the peak at δ 5.03 ppm was assigned to the protons of the amino group. The synthetic steps and reaction conditions for the sulfonated monomer 4-DABS are shown in Scheme 1. The structure of 4-DABS was characterized by its ^{1}H NMR spectra, as shown in Fig. 1b. The peaks at δ 8.92 and 8.81 ppm were assigned to the protons of the hydroxyl groups, while the peak at δ 5.03 ppm for the amino group (in 4-AmPHQ) completely disappeared. The new peaks around δ 3.28, 2.69, 1.63, and 1.39 ppm were assigned to the protons of methylene groups

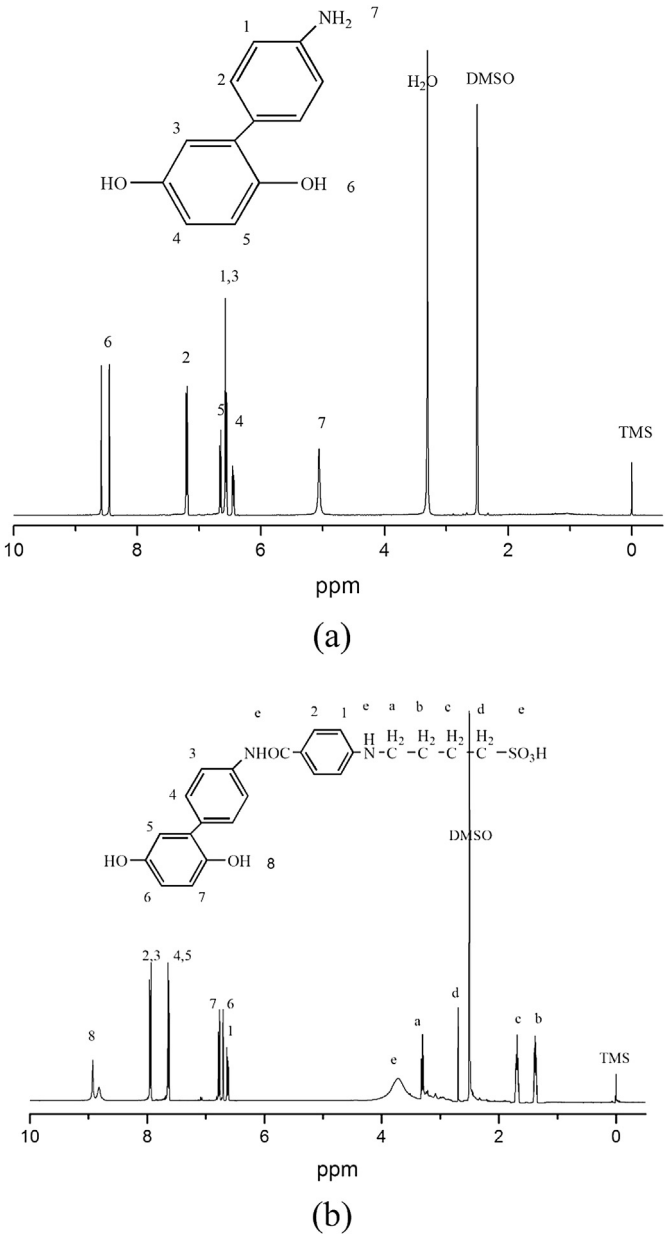

Fig. 1. ^{1}H NMR spectrum of 4-AmPHQ (a) and 4-DABS (b).

(H_a, H_b, H_c, and H_d, respectively). The broad peak at δ 3.83 ppm (H_e) was assigned to the active hydrogen proton in sulfonic acid (SO_3H) group derived from the sulfobutylation, secondary amine groups and amide bond. The ^{1}H NMR spectra of the monomers agree well with their assigned structures, indicating the successful synthesis of 4-DABS.

As shown in Scheme 2, the SPAEK copolymers were synthesized by nucleophilic polycondensation. The structures of the SPAEK copolymers were characterized by their ^{1}H NMR and FTIR spectra. Fig. 2 shows the ^{1}H NMR spectra of the SPAEK copolymers along with peak assignments. The protons H_b, H_c, and H_d in the methylene groups of the SPAEK copolymers appeared at δ 1.31, 1.55, and 2.69 ppm, respectively. The peak for H_a appeared around δ 3.30 ppm, and could not be observed in Fig. 2, as it was obscured by the H_2O peak. The broad peak at δ 4.11 ppm (H_e) was assigned to the active hydrogen proton in the SO_3H groups derived from the sulfobutylation [34], secondary amine groups and amide bond. The peaks at δ 6.58–8.12 ppm were assigned to the protons of phenyl rings. Fig. 3 shows the FT-IR spectra of the SPAEK-100 copolymer. The peaks around 1038 cm^{-1} and 1109 cm^{-1} were assigned to the characteristic O=S=O stretching vibration of the sulfonic acid groups, and the peak at 604 cm^{-1} was assigned to the S–O stretching vibration of the sulfonic acid groups. The peak around 2927 cm^{-1} was assigned to the aliphatic side chain methylene (–CH_2–) groups. The peak at 1654 cm^{-1} was assigned to the carbonyl (C=O) groups in the amide bonds. Thus, the successful synthesis of the SPAEK copolymers was proved by the spectra from the ^{1}H NMR and FT-IR.

The inherent viscosities of the polymers are listed in Table 2. The high viscosity values (1.09–1.21 dL g^{-1}) and good film-forming abilities of the SPAEK copolymers indicate that the polymerizations were carried out successfully and high molecular weight polymers were obtained.

3.2. IEC, water uptake, swelling ratio, and contact angle

IEC is usually defined as the moles of fixed SO_3 sites per gram of polymer. The degree of sulfonation (DS) can be expressed in the form of the IEC. IEC affects the water uptake and proton

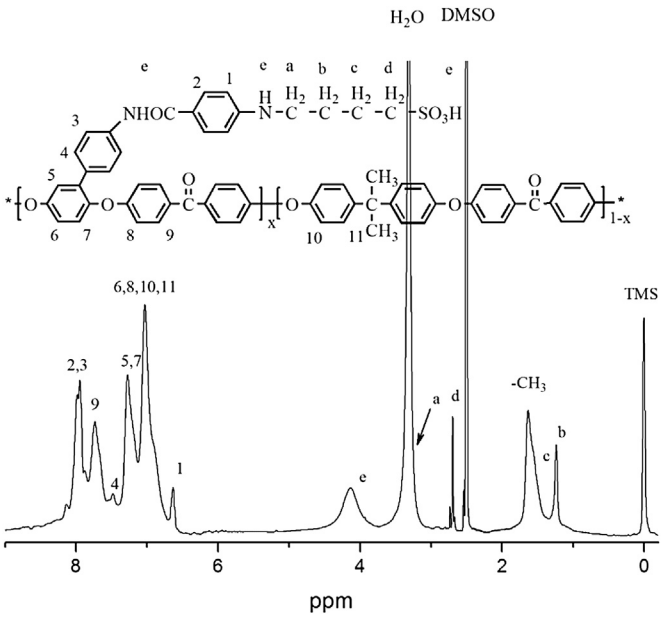

Fig. 2. ^{1}H NMR spectrum of SPAEK copolymer.

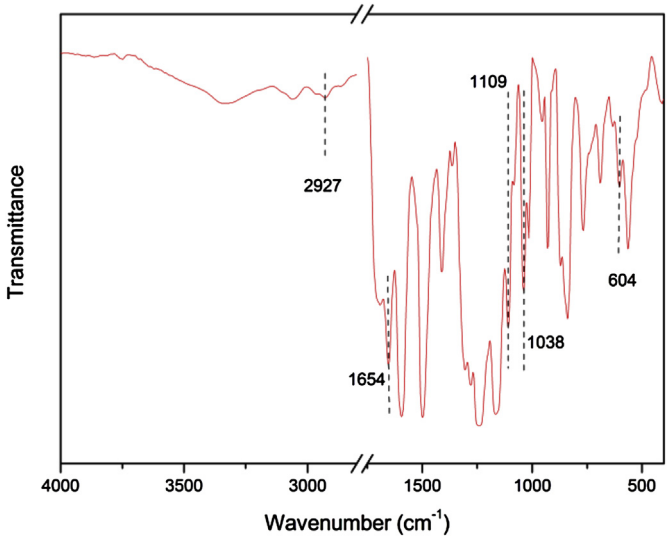

Fig. 3. FT-IR spectra of SPAEK-100 copolymer.

conductivity of the membranes. The IEC values of the SPAEK membranes were in the range of 0.98–1.49 mequiv. g^{-1}, as listed in Table 1. The DS of the SPAEK copolymers was controlled by adjusting the ratio of the sulfonated to unsulfonated monomer feeds. As expected, the IEC values of the SPAEK copolymers increased with increasing DS, which further confirmed that the side chain sulfonic acid groups were introduced to the copolymers via nucleophilic polycondensation.

For most PEMs, water acts as the carrier for proton transportation through the polymeric membranes, due to the fact that protons in the form of hydronium ions ($H_3O^+$and $H_5O_2^+$) in the water are transported by the PEMs through the hydrogen-bonded ionic channels and cationic mixtures [35] Abundant hydration for electrolyte membranes is crucial for high proton conductivity. However, excess water uptake in the polymeric membranes will cause extreme swelling leading to a decrease in their mechanical properties and dimensional stability. The water uptake and swelling ratio were measured from the changes in weight, length and thickness, respectively, between dry and hydrated membranes at the desired temperatures. As expected, water uptake (Fig. 4) and swelling ratio (Fig. 5) of the copolymer membranes both increased as the temperature and IEC increased. All the copolymer membranes, except SPAEK-100 (32.95%, 80 °C), exhibited lower water uptake compared to Nafion 117 (27.9%, 80 °C), although Nafion 117 exhibited a much lower IEC (0.92 mequiv. g^{-1}) [36]. All the copolymer membranes also exhibited lower swelling ratio compared to Nafion 117, particularly at elevated temperatures. The swelling ratio of SPAEK-100 (9.59%, 80 °C) was only about half that of Nafion 117 (17.22%, 80 °C), although SPAEK-100 exhibited higher water uptake. This was probably related to the structure of side chain in SPAEK-xx including aromatic rings, which lead to the structure of the side chain is not as flexible as Nafion 117. As shown in Figs. 4 and 5, all these side-chain-type sulfonated copolymers also exhibited moderate water uptake and a much lower swelling ratio compared to the other main-chain-type sulfonated polymers with similar IEC values, due to the difference in their molecular structures [31,37,38]. Compared to the main-chain-type sulfonated polymers, sulfonic acid groups of the side-chain-type sulfonated polymer are located on the flexible side chains. This different type of molecular structure is advantageous for the aggregation of sulfonic acid groups into larger hydrophilic-ion clusters, which is helpful to separate the hydrophilic sulfonic acid groups from the hydrophobic

Table 1
IEC, contact angle, proton conductivity, methanol permeability, relative selectivity, and water diffusion coefficient of the membranes.

Samples	IEC (mequiv. g^{-1})	Contact angles	Proton conductivity (S cm^{-1})				Methanol permeability (cm^2 s^{-1})		Relative selectivity[a]	Water diffusion coefficient (cm^2 s^{-1})
			25 °C	80 °C	100 °C	120 °C	25 °C	60 °C		
SPAEK-60	0.98	75.9	0.011	0.037	0.065	0.076	0.12×10^{-7}	0.27×10^{-7}	28.74	8.08×10^{-10}
SPAEK-70	1.12	72.6	0.019	0.064	0.089	0.097	0.31×10^{-7}	0.83×10^{-7}	19.21	9.19×10^{-10}
SPAEK-80	1.24	66.1	0.032	0.087	0.111	0.116	0.97×10^{-7}	2.41×10^{-7}	10.34	1.45×10^{-9}
SPAEK-90	1.37	60.7	0.042	0.105	0.128	0.134	2.23×10^{-7}	5.53×10^{-7}	5.90	2.43×10^{-9}
SPAEK-100	1.49	56.3	0.051	0.119	0.144	0.152	3.55×10^{-7}	8.19×10^{-7}	4.50	4.11×10^{-9}
Nafion 117	0.92	59.8	0.076	0.146	0.159	0.139	23.8×10^{-7}	52.6×10^{-7}	1.00	3.94×10^{-7}

[a] Relative selectivity = membrane selectivity/Nafion 117 selectivity (selectivity = [proton conductivity]/[methanol permeability]) at 25 °C.

polymer main chains. Therefore, the water molecules were restricted to the hydrophilic domains and suppressed the effect of water sorption on the hydrophobic polymer main chain, which in turn effectively decreased the water swelling of the membranes [21,22]. In addition, the copolymer membranes become more compact because of the interactions between the nitrogen atoms and sulfonic acid groups [39,40], thereby further increasing the dimensional stability of the membranes, as shown in Scheme 3.

Contact angles are characteristic constants of liquid/solid systems that provide valuable information on the surface energies of solids. In general, the smaller the contact angle against the water, the better the hydrophilicity of the polymer [41,42]. The contact angle measurements were carried out on the smooth surface of the polymer membranes. As shown in Fig. 6 and Table 1, the contact angles of the SPAEK membranes against water decreased with increasing IEC, which indicates that the water uptake increased as the IEC increased. This is consistent with the test results for the water uptake, which also further confirmed that the side chain sulfonic acid groups were successfully introduced into the copolymers.

3.3. Mechanical properties and oxidative stabilities of the SPAEK membranes

Mechanical properties are an important performance index for membrane materials. Sulfonated polymers need to have good mechanical properties before they can be used in proton exchange membranes. The mechanical properties of the SPAEK membranes are listed in Table 2. The tensile strength at maximum load, Young's modulus, and elongation at break of the SPAEK copolymers were in the range of 45.34–53.39 MPa, 1385.64–1576.56 MPa, and 8.85%–13.96%, respectively. The results indicated the side-chain-type SPAEK membranes possessed excellent mechanical properties that are favorable for PEMs.

The oxidative stability of the series of side-chain-type SPAEK membranes was determined by recording the retained weight

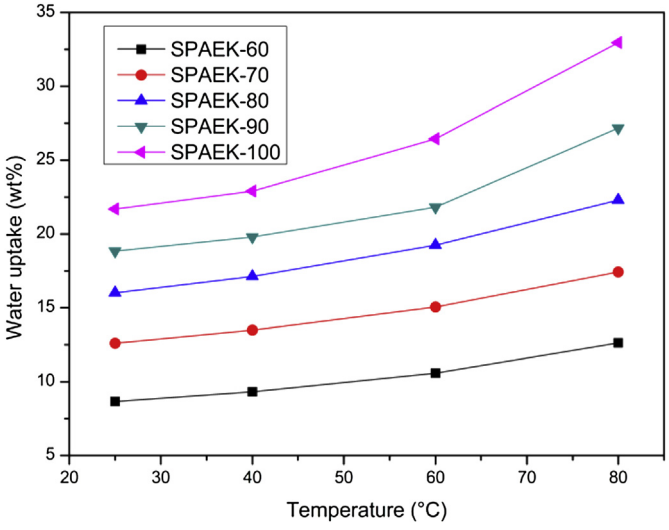

Fig. 4. Water uptake of SPAEK-xx membranes as a function of temperature.

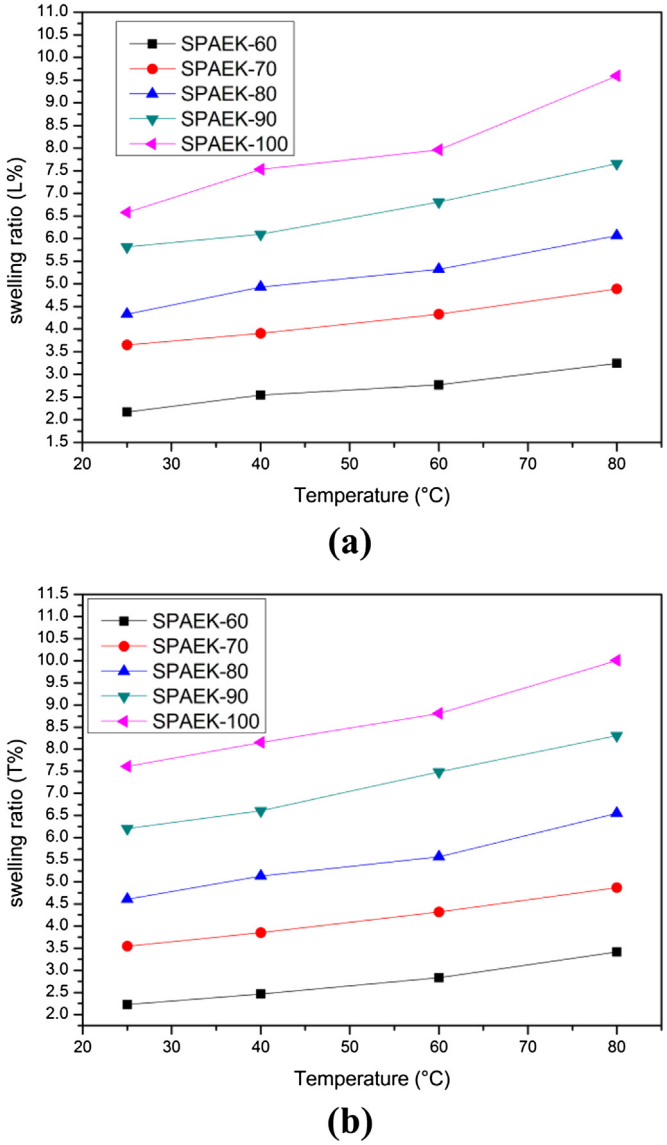

Fig. 5. Water swelling ratio of SPAEK-xx membranes as a function of temperature (a) swelling ratio in length, (b) swelling ratio in thickness.

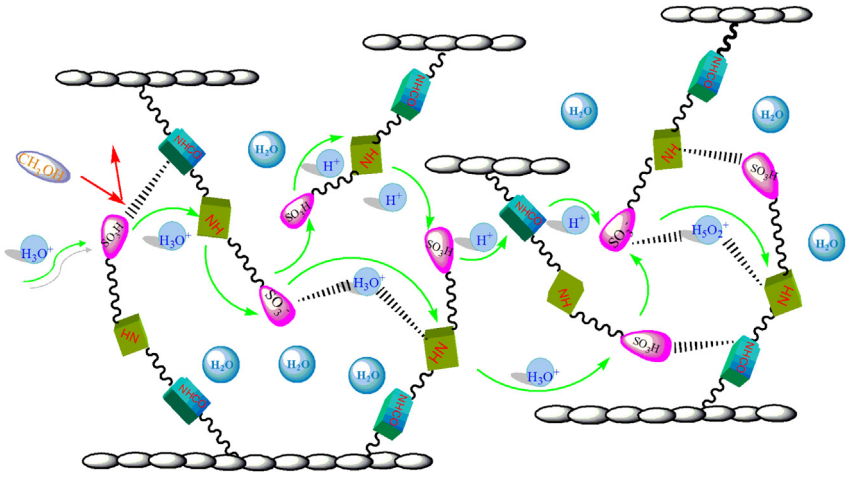

Scheme 3. Schematic structure of the composite membrane.

(RW) after treatment in Fenton's reagent at 80 °C for 1 h. The resistance to oxidation data for the SPAEK membranes is given in Table 2. The resistance to oxidation primarily depends on the water uptake and swelling ratio of the membrane [43]. High water uptake and swelling ratio reduce the density of the polymer molecular chain structure, thereby decreasing the time that free radicals (HO• and HO_2•) can be intruded into the membranes; thus, the membranes' resistance to oxidation was reduced. The resistance to oxidation of the membranes decreased with increasing IEC. As described previously, the differences in molecular structure could effectively inhibit the swelling ratio of the SPAEK membranes. The RW of all the polymer membranes was >91% after treatment with Fenton's reagent (80 °C, 1 h). Therefore, the oxidative stability had not been obvious affected by introducing the benzylic hydrogens into the side-chain-type SPAEK copolymers.

3.4. Thermal properties

The thermal properties of the SPAEK copolymers were analyzed using DSC and TGA, and the results are shown in Figs. 7 and 8. The glass transition temperature (T_g) was not obvious for the acid-form of SPAEK copolymers. The SPAEK copolymers were amorphous and only one T_g was found in their DSC curve (Fig. 7) for every Na-form of the membrane. The T_g values of the copolymers were in the range of 203–229 °C (Table 2) and showed an elevated glass transition with an increase in the sodium sulfonate group. The stability of the side chain sulfonic acid groups was enhanced due to the interactions between the nitrogen atoms and sulfonic acid groups. The 5% weight loss temperatures ($T_{d\ (5\%)}$) of the SPAEK copolymers were all above 267 °C, satisfying the requirement of thermal stability for use in PEMFCs [44]. A typical TGA curve of the SPAEK copolymers is shown in Fig. 8. The initial weight loss of 100–200 °C was attributed to the remaining solvent (NMP) and water being released from the SPAEK copolymers. The second weight loss started at about 240 °C owing to the thermal degradation of the sulfonic acid groups. The third weight loss was observed at about 500 °C owing to the degradation of the polymer main chain.

3.5. Morphology

The hydrophilic-hydrophobic microphase separation structure is closely related to proton conductivity and water uptake in the membranes. A typical TEM image is shown in Fig. 9. The dark regions in the TEM images correspond to the sulfonate ionic clusters stained by silver ions and representing the hydrophilic domains, while the light regions correspond to the hydrophobic regions formed by the hydrophobic polymer backbones. The TEM images indicate that the sulfonate groups aggregated into the hydrophilic clusters, providing proton transport pathways or ionic transport channels [26]. In SPAEK-60, these hydrophilic clusters were randomly dispersed throughout the polymer matrix and no clear phase separation was observed. This suggested a lack of connectivity in the ionic phase in the polymer matrix to form ionic channels. When comparing the SPAEK-100 to SPAEK-60 copolymer, a continuous and larger transport channel in SPAEK-100 copolymer was observed, indicating that a higher sulfonation content in the SPAEK-100 copolymer resulted in more and larger hydrophilic domains, and the wide ion channels could be responsible for the relatively high water uptake and proton conductivity.

3.6. Water retention capacity

The water retention capacity of PEMs is closely related to their proton conductivity, in particular, at high temperatures and low relative humidity. In addition, the water retention capacity of the membranes is very important in view of their application in PEMFC,

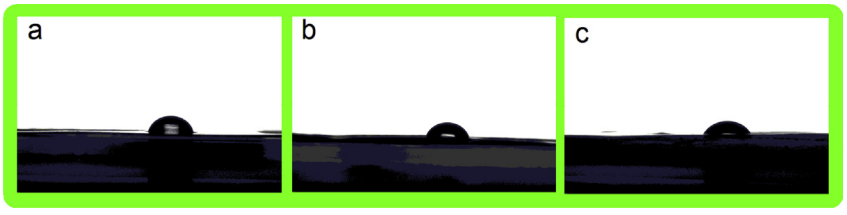

Fig. 6. Pictures of contact angles of SPAEK-60 (a), SPAEK-80 (b), and SPAEK-100 (c) copolymers against water.

Table 2
Mechanical properties, oxidative stability, thermal properties, and inherent viscosities of the polymers.

Samples	Tensile modulus (MPa)	Tensile strength (MPa)	Elongation at break (%)	Oxidative stability (RW %)	$T_{d\ (5\%)}$ (°C)	T_g (°C)	η_{inh}[a] (dL g^{-1})
SPAEK-60	1576.56	53.39	13.96	96	301	203	1.12
SPAEK-70	1518.30	52.09	12.30	96	296	207	1.09
SPAEK-80	1438.80	48.72	11.12	94	291	214	1.15
SPAEK-90	1456.47	49.19	11.96	93	279	223	1.18
SPAEK-100	1385.64	45.34	8.85	91	267	229	1. 21

[a] The inherent viscosities were measured in NMP with a polymer concentration of 0.5 g dL^{-1} at 25.

and could be obtained information from the velocity of water desorption in the membranes. In order to study the water retention capacity of the SPAEK membranes, water desorption coefficients were calculated by measuring the weight loss at 80 °C in 1 h. The desorption isotherm curves are shown in Fig. 10. The plots of M_t/M_∞ versus $t^{1/2}$ initially were linear for Fickian diffusion [45,46]. The diffusion coefficients of the SPAEK membranes were determined from the initial slopes according to Formula (4) and are listed in Table 1. The water diffusion coefficient of the SPAEK membranes increased with increasing IEC, and it may be closely related to the change in the microstructures. As the content of the sulfonated groups increased, the hydrophilic domains became more continuous as well as their density and average size increasing, as seen in Fig. 9. This resulted in an increase in the velocity of water volatilization with the increment of IEC. However, the side-chain-type SPAEK membranes still exhibited lower diffusion coefficients compared to the main-chain-type SPAEK membranes with similar IEC values, as reported previously [31]. As shown in Scheme 3, this result may be attributed to the interactions between the nitrogen atoms and sulfonic acid groups that made the copolymer membranes more compact.

3.7. Proton conductivity and methanol permeability

Proton conductivity is an important property of PEMs and determines their application potential for DMFCs. The proton conductivities of all the acid-forms of the SPAEK hydrated membranes were measured at 25–120 °C in air, and the results are shown in Table 1 and Fig. 11. The proton conductivity of all the SPAEK-xx membranes increased with increasing IEC values and temperature. In general, a conductivity of $>10^{-2}$ S cm^{-1} for PEM materials in fuel cells is required. All the prepared SPAEK membranes showed reasonable proton conductivities $>10^{-2}$ S cm^{-1}. Also, we found that the proton conductivity of Nafion 117 began to decline when temperature over 100 °C. While, the proton conductivity of the SPAEK membranes displayed a little rising trend, and the proton conductivity of the SPAEK-100 was higher than that of Nafion 117 at 120 °C.

The proton conductivities are shown as Arrhenius plots in Fig. 11. The activation energies of the SPAEK membranes were calculated from the slope at 25–80 °C. SPAEK-100 showed an activation energy of about 14.7 kJ mol^{-1}, higher than that of Nafion 117 (9.1 kJ mol^{-1}) [47]; however, it was lower than that of main-chain-type sulfonated aromatic polymers with similar IEC values (about 41.0 kJ mol^{-1}) [48]. Although the SPAEK-xx membranes exhibited higher IEC values than that of Nafion 117 (0.92 mequiv. g^{-1}), all the membranes displayed lower proton conductivities than Nafion 117. This was probably due to the unique ion-rich channels and highly acidic perfluorosulfonic acid that allowed the ion transport more easily, as ion transport requires less activation energy. In addition, the side chains in SPAEK-xx include aromatic rings that will increase the limitation on their mobility due to steric hindrance in comparison to the side chain in Nafion 117. Compared to other main-chain-type sulfonated aromatic polymers with similar IEC values, these side-chain-type SPAEK copolymers exhibited similar or higher proton conductivity with much lower water uptake [31,37,38]. This might be attributed to the following two aspects. (1) The special side-chain-sulfonated structure of the SPAEK copolymers: the sulfonic acid groups attached to the flexible side chains of the polymers could decrease the limitation of rigid polymer backbones on their mobility, forming an appropriate chemical structure for an ionic network and thus improving proton conductivity [49]. The TEM images show the formation of wide and well-connected micellar channels (Fig. 9). (2) The proton conduction mechanism of the SPAEK copolymers under humidified

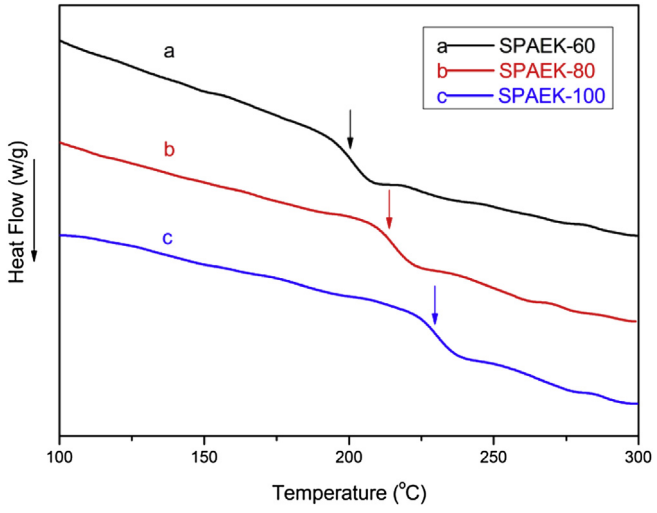

Fig. 7. DSC curves of SPAEK-xx.

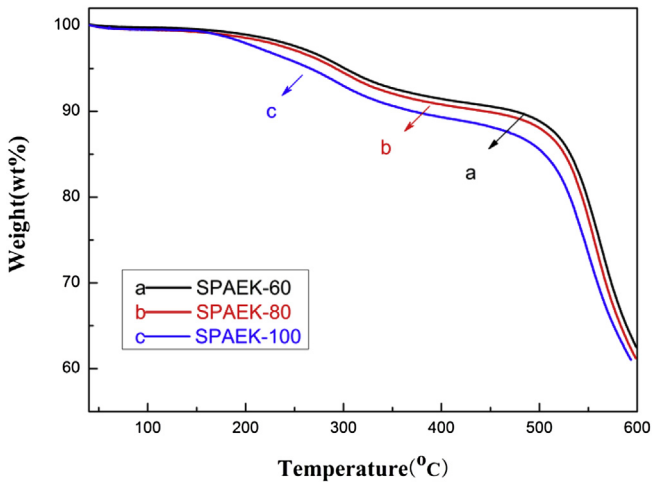

Fig. 8. TGA curves of SPAEK-xx membranes.

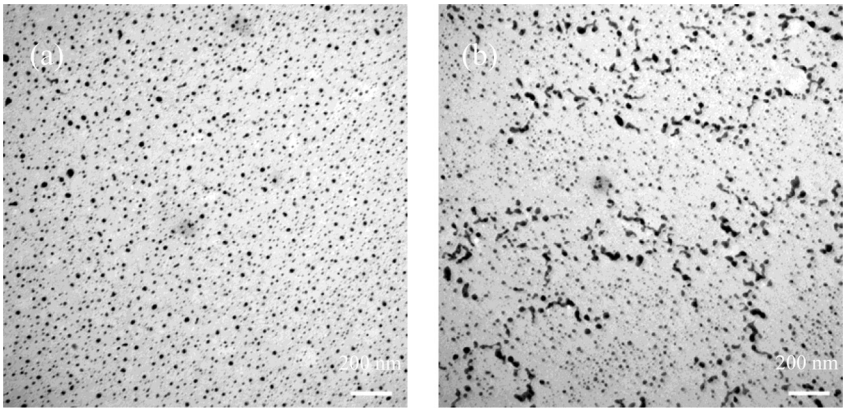

Fig. 9. TEM images of membranes SPAEK-60 (a) and SPAEK-100 (b).

conditions may be attributed to both Grotthuss and vehicle-type mechanisms. The vehicle-type mechanism is possible in the hydrophilic regions where ions (H_3O^+, $H_5O_2^+$, and $H_9O_4^+$) were transported between the clustering of the sulfonic acid groups. While, the Grotthuss-type mechanism is possible in the regions where loose acid–base interactions ($SO_3H\cdots N$ and $SO_3H\cdots(H_2O)n\cdots N$, $n \leq 3$) between the sulfonic acid groups and nitrogen atoms occurred through hydrogen bond formation [39]. The protons diffuse through the hydrogen bond network via the formation and cleavage of hydrogen bonds, thereby facilitating the transport of protons according to the Grotthuss mechanism [21]. The schematic of the side-chain-type SPAEK membranes is shown in Scheme 3.

In DMFCs, the proton conductivity of the membranes directly influenced the performance of the battery, and the methanol permeability determined the efficiency and the service life of the battery. The methanol permeability values for 10 M methanol concentration of SPAEK-xx membranes were measured at 25 and 60 °C (Table 1). The methanol permeability values increased with increasing IEC values and water uptake. The SPAEK-xx membranes exhibited lower methanol permeability in the range of 0.12×10^{-7}–3.55×10^{-7} $cm^2\ s^{-1}$ at 25 °C and 0.27×10^{-7}–8.19×10^{-7} $cm^2\ s^{-1}$ at 60 °C, which were much lower than the value for Nafion 117 (23.8×10^{-7} $cm^2\ s^{-1}$, 25 °C). This might be closely related to the acid–base interaction between the sulfonic acid groups and nitrogen atoms, reducing the vacant space that absorbs free water molecules and inducing a much denser structure to act as the methanol barrier [50]. Membranes intended for use in DMFCs are required to act as both a high proton conductor and an effective barrier to prevent methanol from crossing over. Although these side-chain-type SPAEK membranes showed relatively lower proton conductivity than Nafion 117, their much lower methanol permeability attribute was sufficient to achieve improved DMFC performance. Selectivity is defined as the ratio of the proton conductivity to methanol permeability, which often used to evaluate the potential performance of DMFC membranes. The relative selectivity of the SPAEK-xx membranes was found to be higher than that of Nafion 117, as listed in Table 1, indicating that these side-chain-type SPAEK membranes have great potential for DMFC applications.

3.8. Full cell performance

The fuel cell performances of SPAEK membranes were studied with polarization curves in a single cell test. Fig. 12 displayed the polarization and power density curves for SPAEK 60, 80 and 100 under fully humidified inlet gas conditions ($RH_a/RH_c = 100\%/100\%$) at 100 °C. The fuel cell performance of the SPAEK membranes increased with increasing IEC. The maximum power densities of SPAEK 60, 80, and 100 membranes were roughly 468, 554, 607 mW cm^{-2}, respectively.

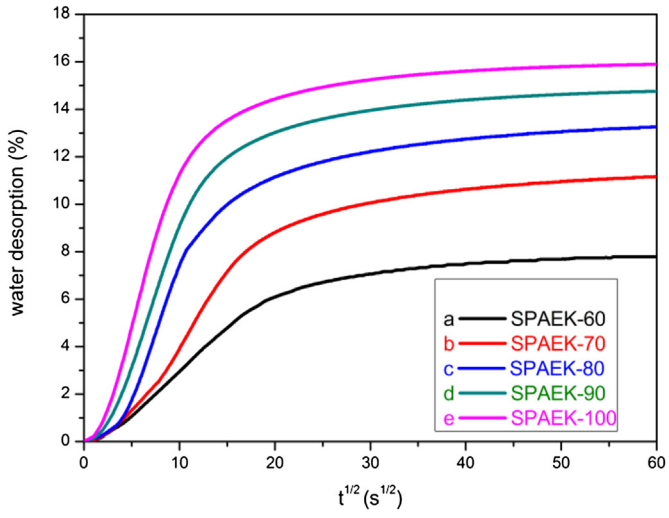

Fig. 10. Water diffusion coefficient of the SPAEK-xx membranes.

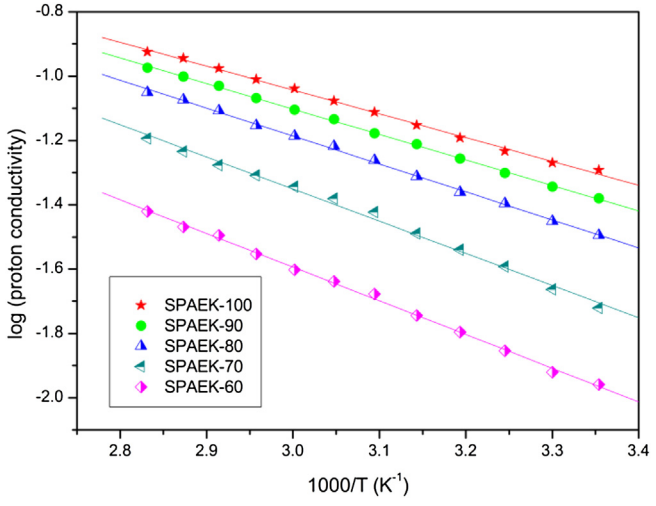

Fig. 11. Proton conductivities of acid-form SPAEK-xx membranes as a function of temperature.

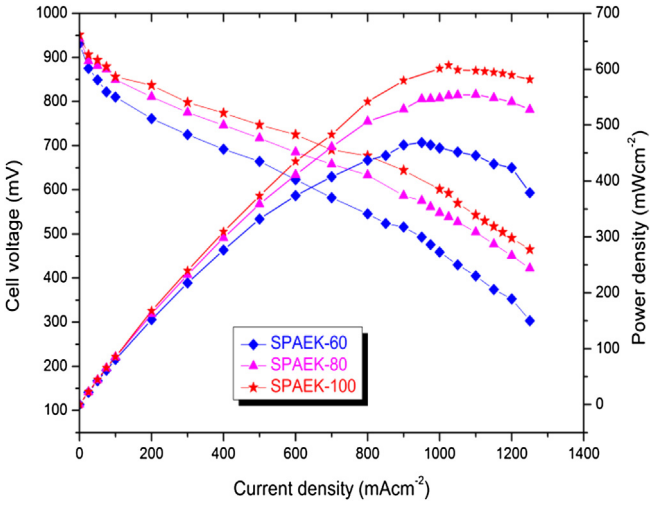

Fig. 12. Polarization curves for SPAEK membranes at 100 °C under 100% RH condition.

4. Conclusion

A series of novel side-chain-type SPAEK copolymers were successfully synthesized and tested as proton conductive materials. The IEC values (0.98–1.49 mequiv. g^{-1}) of the SPAEK copolymers were controlled easily by adjusting the ratio of the sulfonated to unsulfonated monomer feeds. These side-chain-type SPAEK membranes exhibited a desirable mechanical performance as well as excellent oxidative and thermal stabilities. Compared to the main-chain-type sulfonated aromatic polymers with similar IEC values, these side-chain-type SPAEK membranes exhibited relatively low water uptake, low swelling ratio, low methanol permeability, and advantageous proton conductivity owing to their different molecular structure. Although these side-chain-type SPAEK membranes exhibited lower proton conductivity than Nafion 117, they had a higher relative selectivity than that of Nafion 117. All the results obtained in this study suggested that these side-chain-type SPAEK membranes have great potential for application in PEMFCs.

Acknowledgment

The authors would like to thank the National Natural Science Foundation of China (Grant No: 51273024; Grant No: 51303015) and Department of Education of Jilin Province (Grant No: 2012103) for financial support for this work.

References

[1] C.H. Park, C.H. Lee, M.D. Guiver, Y.M. Lee, Prog. Polym. Sci. 36 (2011) 1443–1498.
[2] R.C. Laberty, K. Valle, F. Pereira, C. Sanchez, Chem. Soc. Rev. 40 (2011) 961–1005.
[3] Y. Zhang, X. Fei, G. Zhang, K. Shao, C.J. Zhao, H. Na, et al., Int. J. Hydrogen Energy 35 (2010) 6409–6417.
[4] S.H. Zhou, D. Kim, Electrochim. Acta 63 (2012) 238–244.
[5] M.A. Hickner, H. Ghassemi, Y.S. Kim, B.R. Einsla, J.E. McGrath, Chem. Rev. 104 (2004) 4587–4612.
[6] J.A. Kerres, J. Membr. Sci. 185 (2001) 3–27.
[7] Y. Yang, S. Holdcroft, Fuel Cells 5 (2005) 171–186.
[8] C.H. Shen, M. Pan, Z.F. Hua, R.Z. Yuan, J. Power Sources 166 (2007) 419–423.
[9] M.T. Gencoglu, Z. Ural, Int. J. Hydrogen Energy 34 (2009) 5242–5248.
[10] H. Hu, W. Liu, L. Yang, M. Xiao, S.J. Wang, Y.Z. Meng, et al., Int. J. Hydrogen Energy 37 (2012) 4553–4562.
[11] X.F. Li, H.M. Zhang, Z.S. Mai, H.Z. Zhang, I. Vankelecom, Energy Environ. Sci. 4 (2011) 1147–1160.
[12] M. Yoonessi, T.D. Dang, H. Heinz, R. Wheeler, Z.W. Bai, Polymer 51 (2010) 1585–1592.
[13] T.D. Dang, Z.W. Bai, J. Shumaker, N. Venkatasubramanian, Polymer 51 (2010) 463–468.
[14] K. Matsumoto, T. Higashihara, M. Ueda, J. Polym. Sci. Part A Polym. Chem. 47 (2009) 3444–3453.
[15] Q. Zhang, S.B. Zhang, S.H. Li, Int. J. Hydrogen Energy 36 (2011) 5512–5520.
[16] Y. Yin, Y. Suto, T. Sakabe, S.W. Chen, S. Hayashi, T. Mishima, et al., Macromolecules 39 (2006) 1189–1198.
[17] N.W. Li, Z.M. Cui, S.B. Zhang, S.H. Li, J. Polym. Sci. Part A Polym. Chem. 46 (2008) 2820–2832.
[18] J.A. Mader, B.C. Benicewicz, Macromolecules 43 (2010) 6706–6715.
[19] S. Kang, C.J. Zhang, G.Y. Xiao, D.Y. Yan, J. Membr. Sci. 334 (2009) 91–100.
[20] T.S. Jo, C.H. Ozawa, B.R. Eagar, L.V. Brownell, D. Han, C. Bae, J. Polym. Sci. Part A Polym. Chem. 47 (2009) 485–496.
[21] K.D. Kreuer, S.J. Paddison, E. Spohr, M. Schuster, Chem. Rev. 104 (2004) 4637–4678.
[22] K.D. Kreuer, J. Membr. Sci. 185 (2001) 29–39.
[23] B. Lafitte, M. Puchner, P. Jannasch, Macromol. Rapid Commun. 26 (2005) 1464–1468.
[24] K.A. Mauritz, R.B. Moore, Chem. Rev. 104 (2004) 4535–4586.
[25] B. Lafitte, P. Jannasch, Adv. Funct. Mater. 17 (2007) 2823–2834.
[26] D.S. Kim, G.P. Robertson, M.D. Guiver, Macromolecules 41 (2008) 2126–2134.
[27] B.J. Liu, G.P. Robertson, D.S. Kim, M.D. Guiver, W. Hu, Z.H. Jiang, Macromolecules 40 (2007) 1934–1944.
[28] N. Asano, M. Aoki, S. Suzuki, K. Miyatake, H. Uchida, M. Watanabe, J. Am. Chem. Soc. 128 (2006) 1762–1769.
[29] B.J. Liu, Y. Dai, G.P. Robertson, M.D. Guiver, W. Hu, Z.H. Jiang, Polymer 46 (2005) 11279–11287.
[30] Y.H. Zhao, B.K. Zhu, L. Kong, Y.Y. Xu, Langmuir 23 (2007) 5779–5786.
[31] Z. Wang, C.J. Zhao, H.Z. Ni, H. Na, J. Power Sources 160 (2006) 969–976.
[32] Z. Wang, H.Z. Ni, C.J. Zhao, X.F. Li, T.Z. Fu, H. Na, J. Polym. Sci. Part B Polym. Phys. 44 (2006) 1967–1978.
[33] N. Gao, F. Zhang, S.B. Zhang, J. Liu, J. Membr. Sci. 372 (2011) 49–56.
[34] K. Shao, J. Zhu, C.J. Zhao, Z.M. Cui, Y. Zhang, H. Na, et al., J. Polym. Sci. Part A Polym. Chem. 47 (2009) 5772–5783.
[35] A.A. Kornyshev, A.M. Kuznetsov, E. Spohr, J. Ulstrup, J. Phys. Chem. B 107 (2003) 3351–3366.
[36] Y. Zhang, G. Zhang, Y. Wan, C.J. Zhao, K. Shao, H. Na, et al., J. Polym. Sci. Part A Polym. Chem. 48 (2010) 5824–5832.
[37] P.X. Xing, G.P. Robertson, M.D. Guiver, S.D. Mikhailenko, S. Kaliaguine, Polymer 46 (2005) 3257–3263.
[38] Y. Gao, G.P. Robertson, M.D. Guiver, S.D. Mikhailenko, X. Li, S. Kaliaguine, Macromolecules 37 (2004) 6748–6754.
[39] L. Wu, C.H. Huang, J.J. Woo, S.H. Yun, T.W. Xu, S.H. Moon, et al., J. Phys. Chem. B 114 (2010) 13121–13127.
[40] D.W. Seo, Y.D. Lim, S.H. Lee, Y.G. Jeong, T.W. Hong, W.G. Kim, Int. J. Hydrogen Energy 35 (2010) 13088–13095.
[41] X.J. Zhao, J. Cheng, S.J. Chen, J. Zhang, X.L. Wang, Colloid Polym. Sci. 288 (2010) 1327–1332.
[42] W.Z. Ma, J. Zhang, S.G. Chen, X.L. Wang, Colloid Polym. Sci. 286 (2008) 1193–1202.
[43] C.Y. Tseng, Y.S. Ye, K.Y. Kao, W.C. Shen, J. Rick, B.J. Hwang, et al., Int. J. Hydrogen Energy 36 (2011) 11936–11945.
[44] J.H. Pang, H.B. Zhang, X.F. Li, D.F. Ren, Z.H. Jiang, Macromol. Rapid Commun. 28 (2007) 2332–2338.
[45] T. Watari, J.H. Fang, K. Tanaka, H. Kita, K.I. Okamoto, T. Hirano, J. Membr. Sci. 230 (2004) 111–120.
[46] C.J. Zhao, Z. Wang, D.W. Bi, H.D. Lin, K. Shao, H. Na, et al., Polymer 48 (2007) 3090–3097.
[47] J.H. Pang, H.B. Zhang, X.F. Li, Z.H. Jiang, Macromolecules 40 (2007) 9435–9442.
[48] L. Li, J. Zhang, Y.X. Wang, J. Membr. Sci. 226 (2003) 159–167.
[49] E. Spohr, P. Commer, A.A. Kornyshev, J. Phys. Chem. B 106 (2002) 10560–10569.
[50] N.W. Li, Z.M. Cui, S.B. Zhang, W. Xing, Polymer 48 (2007) 7255–7263.